Inorganic Chemistry

Article

pubs.acs.org/IC

Macrocyclic Dizinc(II) Alkyl and Alkoxide Complexes: Reversible CO_2 Uptake and Polymerization Catalysis Testing

Charles Romain,[†] Michael S. Bennington,[‡] Andrew J. P. White,[†] Charlotte K. Williams,*[,†] and Sally Brooker*[,‡]

[†]Department of Chemistry, Imperial College London, SW7 2AZ London, United Kingdom

[‡]Department of Chemistry and MacDiarmid Institute for Advanced Materials and Nanotechnology, University of Otago, P.O. Box 56, Dunedin 9054, New Zealand

Supporting Information

ABSTRACT: The synthesis of three new dizinc(II) complexes bearing a macrocyclic [2 + 2] Schiff base ligand is reported. The bis(anilido)tetraimine macrocycle reacts with diethylzinc to form a bis(ethyl)dizinc(II) complex, [$L^{Et}Zn_2Et_2$] (**1**). The reaction of complex **1** with isopropyl alcohol is reported, forming a bis(isopropyl alkoxide)dizinc complex, [$L^{Et}Zn_2(^iPrO)_2$] (**2**). Furthermore, complex **1**, with 2 equiv of alcohol, is applied as an initiator for racemic lactide ring-opening polymerization. It shows moderately high activity, resulting in a pseudo-first-order rate coefficient of 9.8×10^{-3} min^{-1}, with [LA] = 1 M and [initiator] = 5 mM at 25 °C and in a tetrahydrofuran solvent. Polymerization occurs with good control, as evidenced by the linear fit to a plot of molecular weight versus conversion, the narrow dispersities, and the limited transesterification. The same initiating system is inactive for the ring-opening copolymerization of carbon dioxide (CO_2) and cyclohexene oxide at 80 °C and 1 bar of CO_2 pressure. However, stoichiometric reactions between complex **2** and CO_2, at 1 bar pressure, result in the reversible formation of new dizinc carbonate species, [$L^{Et}Zn_2(^iPrO)(^iPrOCO_2)$] (**3a**) and [$L^{Et}Zn_2(^iPrOCO_2)_2$] (**3b**), and the reaction was studied using density functional theory calculations. All of the new complexes, **1**−**3b**, are fully characterized, including NMR spectroscopy, elemental analysis, and single-crystal X-ray diffraction.

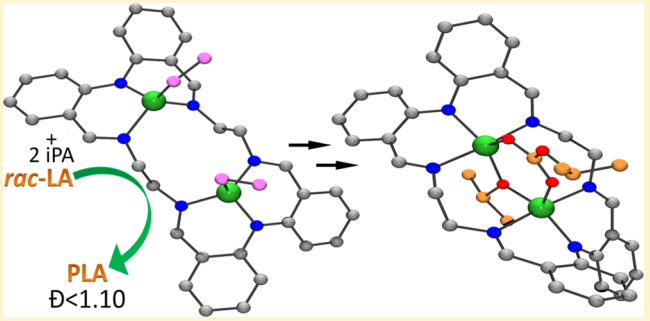

INTRODUCTION

The synthesis of dinuclear zinc(II) complexes is relevant for an understanding of the coordination chemistry and for applications as models for the active sites for various metalloenzymes or in catalysis.[1−7] In polymerization catalysis, dizinc complexes have proven to be highly effective for both ring-opening polymerization (ROP) of lactones and ring-opening copolymerization (ROCOP) of carbon dioxide (CO_2) with epoxides.[8−18] Both processes are societally relevant because they enable renewable resources to be used in the synthesis of useful, commodity materials. In the case of lactide polymerization, the monomer derives from lactic acid, which is harvested from various plants, including sugar cane, maize, and rice.[14,15] The product, polylactide (PLA), is attracting considerable commercial attention as a renewable alternative to petrochemicals, such as polyolefins, for applications in packaging, fibers as well as for specialist medical applications.[19] A recent review highlights some current challenges and opportunities in PLA catalysis.[20] ROCOP of CO_2 and epoxides is also a sustainable process because it allows the partial replacement of epoxides,[8−18] which have a high embedded energy, with CO_2, resulting in a lowering of the environmental footprint for the product polyols.[21] It has recently been shown that CO_2 captured from a power station can be applied in the process.[22] The polyols are proposed to be suitable for use in the preparation of polyurethanes, which are ubiquitous in foam, adhesive, and elastomer applications. Both polymerizations require the application of an initiator, which mediates the rate, selectivity, and properties of the resulting materials.[8−18]

Currently, some of the most promising initiators for these polymerizations are homogeneous dinuclear zinc complexes, due, in part, to high rates of reaction, good selectivities, and favorable properties of the metal ion, including a lack of color, redox chemistry, relatively high abundance, and lower toxicity. Considering the CO_2/cyclohexene oxide ROCOP, the first reports describing zinc complexes date back to the inception of the field and the use of diethylzinc, with protic reagents, to prepare in situ the so-called "initiating system".[23,24] Such systems are ill-defined mixtures of zinc alkyl, hydroxide, and cluster complexes; they showed low rates. In the intervening decades, many better and well-defined homogeneous complexes have been reported. For example, Darensbourg and co-workers pioneered the application of zinc phenolate catalysts, which showed moderate rates but could be fully characterized.[25−27] Coates and co-workers made a major advance when

Received: September 6, 2015
Published: December 1, 2015

DOI: 10.1021/acs.inorgchem.5b02038
Inorg. Chem. 2015, 54, 11842−11851

Chart 1. Selected Examples of Dinuclear Zinc Complexes for Epoxide/CO_2 Copolymerization[28,30,38,39]

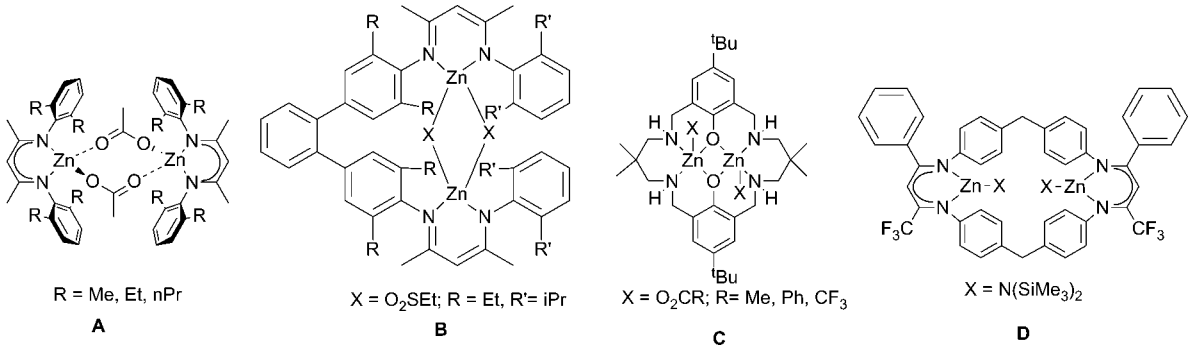

Chart 2. Selected Examples of Dizinc Catalysts for Lactide ROP

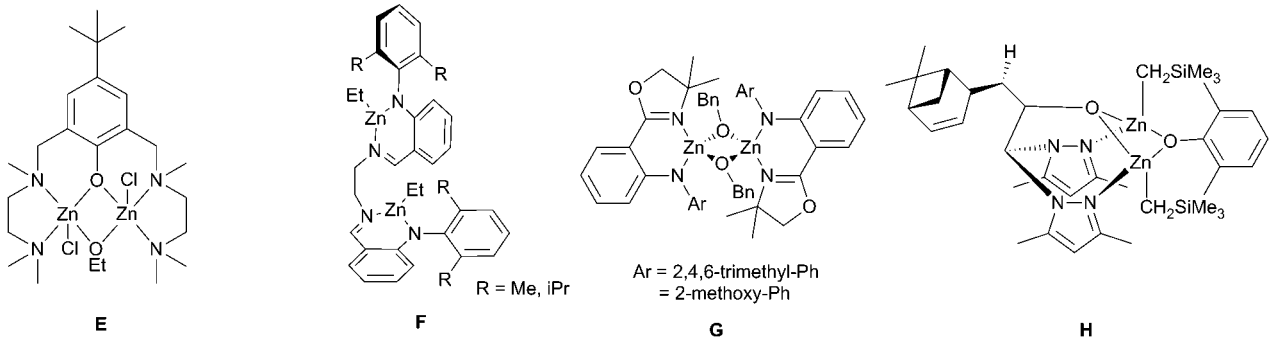

they reported single-site zinc β-(diiminate) complexes, **A** (Chart 1), the best of which has a turnover frequency (TOF) of 730 h^{-1} (7 bar, 50 °C).[28] In a detailed study of the initiator kinetics, it was proposed that the most active catalysts are loosely associated dimeric complexes and that a dinuclear mechanism may be operative.[28] In 2005, Lee and co-workers reported bis(anilido)aniline dizinc complexes, **B** (Chart 1), which showed a TOF of 290 h^{-1} (12 bar, 80 °C).[29,30] In 2009, some of us reported a dizinc macrocyclic complex, **C** (Chart 1), which showed a moderate TOF of 25 h^{-1} (1 bar, 80 °C) but was able to operate at just 1 bar of CO_2 pressure.[31−38]

Subsequently, we have investigated various other metal complexes of this macrocycle and shown that high TOF values of ∼5000 h^{-1} can be obtained using dimagnesium catalysts.[22] A number of researchers tethered together zinc β-diiminate complexes in order to overcome the entropy limitations of dimeric catalysts.[39−43] The geometry and structure of the tethering group were shown to be very important, with a number of well-characterized complexes being reported by various groups as unreactive,[44] while Rieger and co-workers proposed that using flexible tether groups was important.[39,41,42] Indeed, earlier this year, Rieger and co-workers optimized the design strategy for such tethered β-diiminate catalysts, **D** (Chart 1), and were able to record a "record-breaking" TOF of 155000 h^{-1} (30 bar, 100 °C).[39] Thus, there is considerable interest and potential for the development of new dizinc catalysts and, in particular, to understand the requirements at both the metal ions and ancillary ligands to prepare highly active and selective catalysts. Another important area in this field of catalysis is to attempt to isolate and structurally characterize new dizinc complexes and study the elementary reactions proposed to occur in catalysis; therefore, new dizinc alkoxide and carbonate complexes are important targets for reactivity studies.

A range of different dizinc catalysts have also been reported for *rac*-lactide (*rac*-LA) ROP.[11,13,45] An early example of a dizinc catalyst, from Tolman and co-workers, showed high activity and used a phenolate tetraamine ligand scaffold, **E** (Chart 2).[46] Mu and co-workers reported flexibly linked bis-bidentate anilidoaldimine-coordinated ethylzinc(II) complexes, **F** (Chart 2), which were effective initiators of polymerization of ε-caprolactone (ε-CL) in the presence of benzyl alcohol.[47] Chen and co-workers reported dizinc(II) complexes of diphenylamine-based anilidooxazolinate ligands, **G**, as active initiators for L-LA and ε-CL ROP.[48] Otero and co-workers reported the chiral dizinc complexes, **H** (Chart 2), which showed good heteroselectivity in *rac*-LA ROP (P_s = 0.77).[49]

Thus, the recent literature in both ROCOP of epoxides/CO_2 and ROP of lactide demonstrates the potential for dinuclear zinc complexes as catalysts. There is considerable scope for the development of new ligand scaffolds that direct dizinc coordination and that may yield further insight into the features required for successful catalysis.

RESULTS AND DISCUSSION

Here, a 22-membered Schiff base macrocycle, H_2L^{Et} (Figure 1), featuring tetraimine and diphenylamine moieties, was selected for investigation because some of us had reported success in forming dinuclear complexes with transition metals, research done with the expectation that such macrocycles could be a good scaffold for new generations of dinuclear catalysts.[50] The ligand was synthesized via the [2 + 2] condensation of diphenylamine-2,2′-dicarboxaldehyde with diaminoethane, according to the methods previously reported.[50−52] Previously, this type of macrocycle was shown to form dinuclear complexes, and related smaller macrocycles to form mononuclear complexes, whereby the diphenylamine NH moieties

DOI: 10.1021/acs.inorgchem.5b02038
Inorg. Chem. 2015, 54, 11842−11851

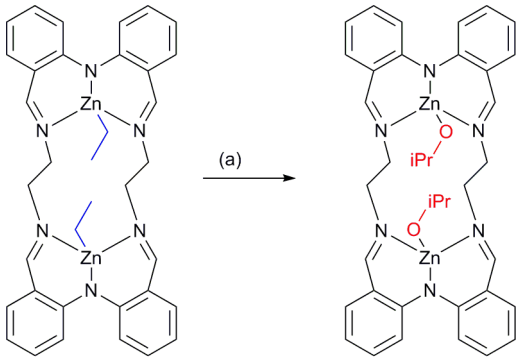

Figure 1. Synthesis of dinuclear zinc complex **1**. Reagents and conditions: (a) 2 Et_2Zn, THF, −40 to +25 °C, 16 h.

are deprotonated, with metal ions including zinc(II), copper(II), nickel(II), iron(II), and cobalt(II).[50,51,53−56]

However, most of these previous complexes either have been cationic species or were prepared in aqueous media: both features are unsuitable for polymerization catalysis. Hence, our approach here was to deliberately target neutral dizinc complexes of the form $[L^{Et}Zn_2X_2]$, where X is a suitable initiating group for polymerization, such as an alkyl, alkoxide, or carbonate group. Zinc(II) was selected because of its strong precedence in various ROP and ROCOP catalyses and for ease of complex characterization.

In order to prepare anhydrous dizinc(II) complexes, $ZnEt_2$ was selected as a suitable reagent because it both enables clean in situ deprotonation of the aniline groups (releasing ethane gas) and delivers the desired ethylzinc(II) moiety to the resulting anionic N_3-donor coordination "pocket". The addition of 2 equiv of $ZnEt_2$ to a suspension of the macrocycle, in tetrahydrofuran (THF), led to clean formation of a dizinc bis(alkyl) complex, $[L^{Et}Zn_2Et_2]$ (**1**), in high yield (87%) (Figure 1). The ^{1}H NMR spectrum (25 °C, C_6D_6) of **1** is consistent with the formation of two rigid (N,N,N)-zinc chelates. Some notable features of the ^{1}H NMR spectrum include (a) the complete absence of signals assigned to the NH proton (δ_{NH} = 11.90 ppm; Figure S4) consistent with the formation of anilido donors, (b) a significant shift of the resonance assigned to the imine protons to lower chemical shifts, consistent with all four imines being coordinated to the two zinc(II) centers (from 8.28 ppm for H_2L to 7.36 ppm for **1**), and (c) a highly symmetric solution structure, indicative of a C_4 symmetric complex. In fact, the ^{1}H NMR spectrum shows one imine resonance, four aromatic resonances, two multiplets for the diasterotopic methylene protons on the linker group and equivalent ethyl groups (Figures S1−S3). In contrast, the ^{1}H NMR spectrum in THF-d_8 (25 °C) indicates that there are two isomeric complexes, present as major (∼85%) and minor (∼15%) species; both show highly symmetric structures. This is tentatively attributed to the coordination of THF at the zinc centers, leading to different ligand conformations (Figure S5). Variable-temperature (VT) ^{1}H NMR analyses over the range −80 and +70 °C showed a significant broadening of all of the ligand signals at around −60 °C, suggesting that there may be an equilibrium between the two isomers (Figure S6). Next, it is important to establish the thermal stability of **1** because polymerization will be conducted at 80 °C. Thus, a solution of **1** (C_6D_6) was maintained, under an inert atmosphere, at 80 °C for 16 h. No significant changes to the ^{1}H NMR spectrum were observed. This is rather different from the results reported by Dagorne and co-workers for [(BIAN)ZnEt] complexes, where the addition of ethyl groups to the ligand imine moieties was observed.[57] In this case, the macrocyclic complex showed good stability and thus has the potential to be applied as a polymerization catalyst.

X-ray Crystallography. Dark-orange crystals of complex **1**·C_6H_6 were obtained by hexane diffusion into a benzene solution, and the structure was determined (Figure 2).

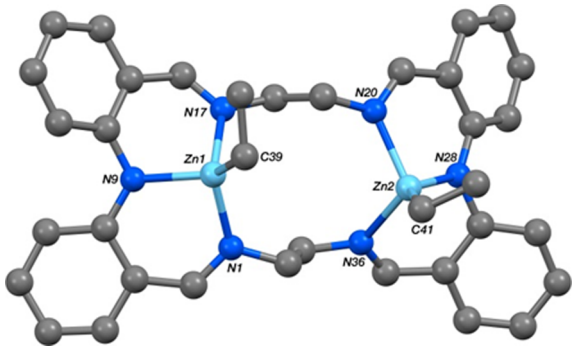

Figure 2. Molecular structure of **1** (for clarity, hydrogen atoms and benzene of solvation are not shown).

The two zinc(II) centers are coordinated in the two tridentate N_3-donor "pockets" of the macrocycle, with each bound to a deprotonated secondary amine nitrogen atom (N_{amine}) and the two flanking imine nitrogen atoms (N_{imine}). Each zinc center is also coordinated to the ethyl ligand, giving overall a CN_3-donor environment. In contrast to the solution structures, the macrocycle binds the zinc(II) centers slightly asymmetrically, with one longer [2.119(2) and 2.103(2) Å] and one shorter [2.022(2) and 2.041(2) Å] Zn−N_{imine} bond. As anticipated, the zinc(II) centers exhibit somewhat distorted tetrahedral coordination environments, with τ_4 = 0.78 and 0.80.[58] This contrasts with the copper(II) centers in the previously reported $[L^{Et/Pr/Bu}Cu^{II}_2(OAc)_2]$ derivatives (22-, 24-, and 26-membered, respectively), which have τ_4 = 0.31−0.41, consistent with distorted square-planar geometries.[50] In the solid-state structure of **1**, the macrocycle retains a flat overall conformation, and the two zinc(II) centers sit above their respective N_3-donor planes, on the same side of the macrocycle, by 1.009 Å (Zn1) and 1.022 Å (Zn2). Because of the flat macrocycle conformation, the Zn−Zn distance is 5.0270(4) Å, whereas the Cu−Cu distance was 3.6072(8) Å in the more folded $[L^{Et}Cu^{II}_2(OAc)_2]$ complex, showing the high flexibility and adaptability to different metal centers of this macrocyclic ligand. Recently, Rieger and co-workers have reported a series of flexibly tethered bis(β-diiminate) dinuclear zinc complexes, some of which show unprecedented high activities in CO_2/epoxide copolymerization catalysis (Chart 1).[39,41,42] In the solid-state structure reported for one of those catalysts, there is a large intermetallic separation, 7.7 Å; however, calculations have shown that the flexibility of the ligand allows separations of 5−5.5 Å to be achieved for some of the key proposed polymerization intermediates.[41] In our previous work, using phenolate or thiophenolate macrocycle ancillary ligands, the solid-state structures show Zn−Zn separations of 3.03[34] or 3.33−3.37 Å.[59,60]

Polymerization Catalysis. Complex **1** was tested for activity in CHO/CO_2 copolymerization reactions, using 2 equiv

DOI: 10.1021/acs.inorgchem.5b02038
Inorg. Chem. 2015, 54, 11842−11851

of alcohol as the initiating group. The polymerizations were run at 1 bar of CO_2 pressure and 80 °C and in neat CHO (catalyst loading of 0.1 mol %). However, under these conditions, only the starting epoxide was observed (Table S1).

Dinuclear zinc(II) complexes have also previously been reported for ROP of cyclic esters;[45−48,61] therefore, **1** was also tested for ROP of *rac*-LA (Figure 3 and Table 1). Complex **1**

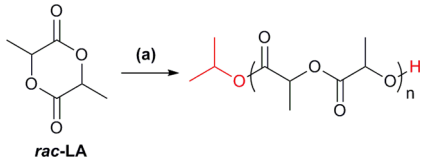

Figure 3. ROP of *rac*-LA initiated by **1**. Reagents and conditions: (a) catalyst **1** (1 equiv), isopropyl alcohol (2 equiv), *rac*-LA (200 equiv), THF, 25 °C, and 80 min.

Table 1. Selected Bond Lengths (Å) and Angles (deg) for Complexes 1, 2, 3a-I, and 3a-II

	1	2	3a-I	3a-II[a]
Zn1−N1	2.0223(17)	2.180(2)	2.166(3)	2.160(2)
Zn1−N9	2.0050(18)	2.013(2)	1.986(2)	2.020(3)
Zn1−N17	2.1186(16)	2.187(2)	2.200(3)	2.160(3)
Zn2−N20	2.0409(17)	2.191(2)	2.179(2)	
Zn2−N28	1.9994(18)	2.011(2)	1.997(2)	
Zn2−N36	2.1033(18)	2.209(2)	2.154(2)	
Zn1−C39	1.991(2)			
Zn2−C41	1.988(4)			
Zn1−O40		1.9897(16)	1.972(2)	*b*
Zn2−O40		1.9884(16)	1.974(2)	*b*
Zn1−O50		1.9835(16)	2.040(3)	*b*
Zn2−O50		1.9795(16)		
Zn2−O52			2.056(3)	*b*
N1···N17	3.386(2)	4.349(3)	4.363(4)	4.319(4)
N20···N36	3.352(2)	4.386(3)	4.329(3)	
N9···N28	8.339(3)	6.960(3)	7.175(3)	7.330(5)
Zn···Zn	5.0270(4)	2.9448(4)	3.2062(5)	3.3337(8)

[a]Because of symmetry, the numbering scheme for **3a-II** is inconsistent with the other complexes, so the closest equivalent alternatives have been used. [b]Bond lengths unreliable because of disorder; see the Supporting Information for more details.

showed good activity using 2 equiv of isopropyl alcohol, at a 1 M concentration of *rac*-LA in THF, 5 mM concentration of catalyst (1:200 loading catalyst/lactide), and 25 °C. The complex was an efficient catalyst, converting >78% of *rac*-LA to polymer within ∼1 h at room temperature. The atactic PLA had a molecular weight (MW) in close agreement with the value predicted on the basis of the catalyst concentration, assuming that both zinc sites initiate chain growth, and the MW distribution was narrow ($Đ$ < 1.10).

The matrix-assisted laser desorption ionization time-of-flight (MALDI-ToF) spectrum of the resulting PLA confirmed the absence of significant transesterification side reactions, as shown by a single series of peaks separated by 144 amu, corresponding to *rac*-LA units (Figure S7). The spectrum also confirmed the isopropoxide chain end group, in accordance with a coordination−insertion mechanism. The polymerization was monitored by taking regular aliquots; there was a linear correlation between the PLA molecular weight (M_n) and monomer conversion (Figure 4), with the experimental molecular weight closely matching the theoretical value. The plot of $\ln([LA]_0/[LA]_t)$ versus reaction time, monitored from 20 to 80% monomer conversion, shows a linear fit, in accordance with a first-order dependence of the rate on the monomer concentration (Figure 4). The gradient represents the pseudo-first-order rate coefficient, $k_{obs} = 9.8 \times 10^{-3}$ min^{-1}, the value of which is within the range observed for other good/fast catalysts, under the same conditions.[10,11,22] The catalyst does show a clear induction period, from 0 to 20% conversion, during which there would be a nonlinear fit to the data. It is proposed that, during this period, formation of the alkoxide species occurs at a rate concurrent with polymerization, indeed such effects have been observed by others in *rac*-LA ROP.[62,63]

Zinc Alkoxide Complex. In order to get a better understanding of the behavior of complex **1** in both polymerization studies, formation of the true propagating species was targeted. In *rac*-LA ROP, the propagating species is proposed to be a zinc alkoxide derivative, formed in situ by reaction with alcohol, while for the CO_2/CHO ROCOP, the intermediates would be zinc alkoxide and carbonate species. Initially, the reaction of **1** with isopropyl alcohol (^{i}PrOH) to form the alkoxide initiating group was studied (Figure 5). Whereas **1** slowly reacts with ^{i}PrOH (2.2−10 equiv vs **1**) in THF or C_6D_6 at 25 °C, upon heating of the mixture to 60 °C, there is essentially quantitative formation of the corresponding alkoxide derivative, $[\mathbf{L}^{Et}Zn_2(^iPrO)_2]$ (**2**), as determined by ^{1}H NMR spectroscopy (Figure S8).

Interestingly, ^{1}H NMR spectroscopic monitoring of the reaction showed that, at room temperature, there were new signals around 12.0 ppm, attributed to the formation of NH moieties and consistent with the alcohol protonating the ancillary ligand rather than reacting with the zinc-bound alkyl groups. This is in line with the remaining characteristic high field signals attributed to the zinc-coordinated ethyl groups, at 0.41 ppm; only minor traces of ethane (0.85 ppm) can be observed. After heating of the reaction to 60 °C for 2 h, there was quantitative conversion to a single product, along with the formation of significant quantities of ethane. The ^{1}H, ^{13}C, and ^{1}H−^{13}C HSQC/HMBC spectra (Figure S10) are consistent with the product being the dizinc bis(isopropoxide) complex **2** (Figure 5). The ^{1}H NMR spectrum shows the expected ligand signals, with significant broadening of the methylene signals in the tether group, as well as signals characteristic of the zinc-coordinated isopropoxide group (3.8, 0.60 and 0.61 ppm). The ^{13}C NMR spectrum confirms the assignment of the alkoxide signals (63.4 and 28.1 ppm). Complex **2** has a high symmetry in solution, with just one peak being observed for the imine protons plus four aromatic signals. In addition, signals characteristic of the NH moieties are absent. On the basis of the in situ NMR monitoring, it is proposed that the zinc alkoxide derivative **2** forms by a two-stage process in which the initial reaction with alcohol protonates the anilido group, and in the second step, intramolecular deprotonation of the NH moiety by the zinc-bound ethyl group occurs. Complex **2** can be successfully synthesized in THF and isolated on a preparative scale in 30% yield. The molecular structure of **2** (Figures 5 and 6) has been confirmed by X-ray diffraction (XRD) studies on crystals obtained by hexane diffusion in a THF solution.

All bonding and geometrical parameters for complex **2** (Table 1) are as expected and are in line with those of the structure of complex **1**. Each of the two zinc(II) centers is contained in a tridentate N_3 binding pocket, binding through

DOI: 10.1021/acs.inorgchem.5b02038
Inorg. Chem. 2015, 54, 11842−11851

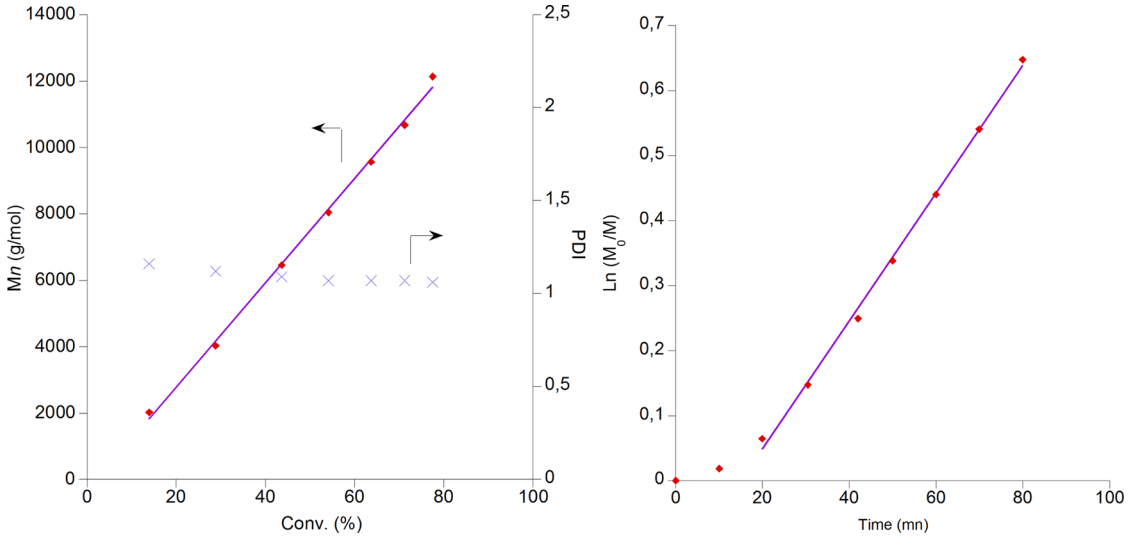

Figure 4. Plots of *Mn* versus *rac*-LA conversion (left) and $\ln(M_0/M)$ versus time. Reaction conditions as per Figure 3.

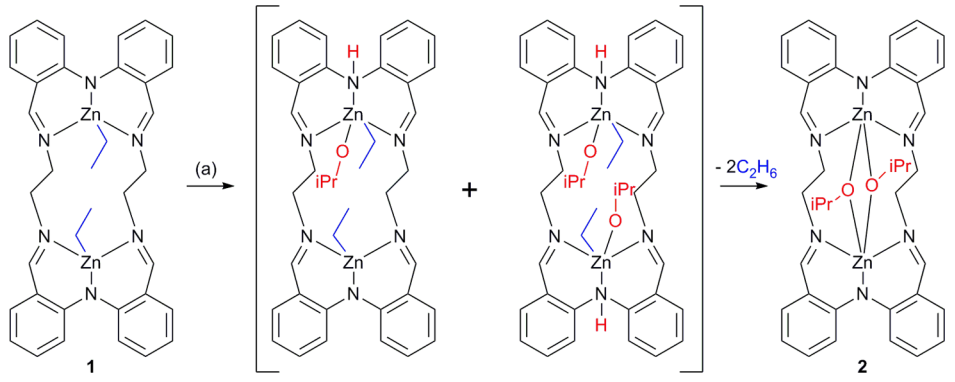

Figure 5. Reaction of complex **1** to form the bis(isopropoxide) complex **2** (some possible intermediates also shown). Reaction conditions: (a) isopropyl alcohol, THF, or C_6D_6, 16 h, and 60 °C.

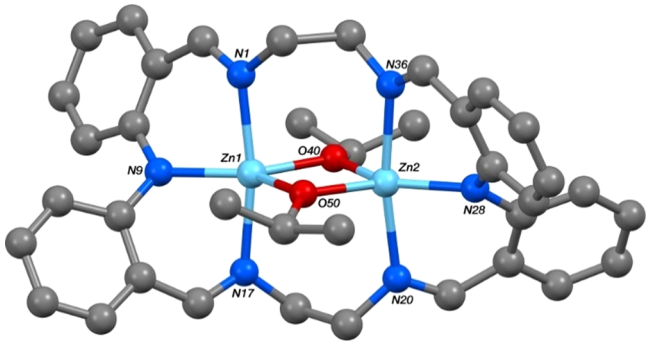

Figure 6. Molecular structure of **2**.

the deprotonated amine and two imine nitrogen atoms. The zinc(II) centers are also coordinated to two μ^2-bridging oxygen atoms from the two isopropoxide ligands, leading to distorted five-coordination N_3O_2-donor environments (τ_5 = 0.47 and 0.48).[64] Interestingly, complex **2** features a more planar central structure than complex **1**, with the zinc(II) centers lying close to their respective N_3 planes (0.020−0.075 Å out-of-plane compared to 1.009−1.022 Å) and the two N_3 planes inclined by only ca. 10.6−15.2° compared to 28.5° in **1**.

Zinc Carbonate Complex. ROCOP of CHO/CO_2 was not found to be successful using catalyst **1** with 2 equiv of alcohol. It is expected that complex **1** reacts with isopropyl alcohol, under the conditions of catalysis (80 °C), to yield the alkoxide derivative **2**, from which propagation can occur. Thus, it was of interest to establish the reactivity of complex **2** toward

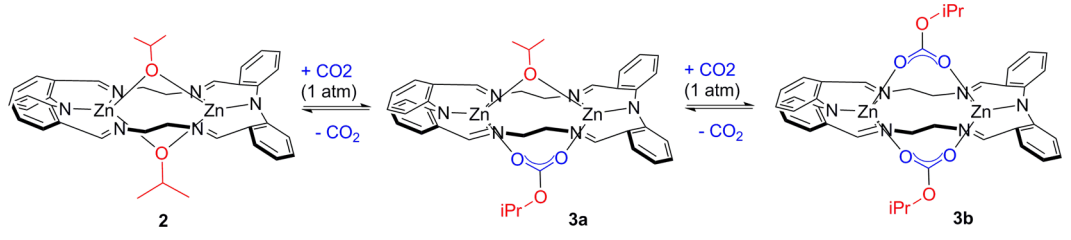

Figure 7. Formation of zinc carbonate complexes from **2** via CO_2 insertion.

DOI: 10.1021/acs.inorgchem.5b02038
Inorg. Chem. 2015, 54, 11842−11851

CO_2. It should be mentioned that there are still only a few studies of the fundamental reactivity of zinc alkoxide derivatives toward CO_2 and that isolated examples of zinc carbonate complexes are rare.[28,65−67] Thus, in order to gain insight into one of the key propagating steps in catalysis, the reactions between **2** and CO_2 were studied (Figure 7). ^{1}H NMR spectroscopic monitoring of the reaction of **2** with CO_2, at 1 atm of pressure, in C_6D_6 and at 25 °C, leads to the rapid disappearance of the alkoxide complex signals and the evolution of new signals, assigned to zinc carbonate species (Figure S11). Although there are several species present at the end of the reaction (Figure S11), the major compound is assigned to be a dizinc bis(carbonate) complex, **3b**, the structure of which is illustrated in Figure 7. For this major species, there is a significant shift in the resonances associated with the isopropoxide group compared to those for the starting alkoxide species, from 3.80 ppm (alkoxide compound **2**) to 4.47 ppm (carbonate compound **3b**), as well as a notable shift to lower values for the imine protons (from 8.32 ppm for **2** to 7.72 ppm for **3b**). The ^{13}C NMR spectrum also shows a significant shift in the resonance attributed to the isopropoxide group (from 65.2 ppm for **2** to 69.4 ppm for the carbonate species **3b**). Further, a new quaternary carbon signal at 157.8 ppm is observed, in accordance with the formation of a carbonate group. VT ^{1}H NMR spectroscopy, monitored over the range of 25−80 °C, indicates that there are other species in equilibrium with **3b**, particularly at higher temperatures (Figure S11).

It should be noted that, because of the flexibility of the ligand and the different coordination modes of the carbonate groups (Figure S13), it is difficult to unambiguously confirm the formation of only **3b**; certainly, the presence of some **3a** cannot be excluded. Nevertheless, at higher temperatures, the ^{1}H and 2D NMR spectra give much clearer indications that **3a** is present, most clearly by the evolution of a new signal at 3.66 ppm, which is characteristic of the isopropyl groups of an alkoxide species (see Figure S11). It was possible to isolate crystals from the mixture, and an XRD study confirmed that the species was the zinc carbonate−alkoxide complex **3a** (Figure 8). It is important to note that the crystals were obtained under

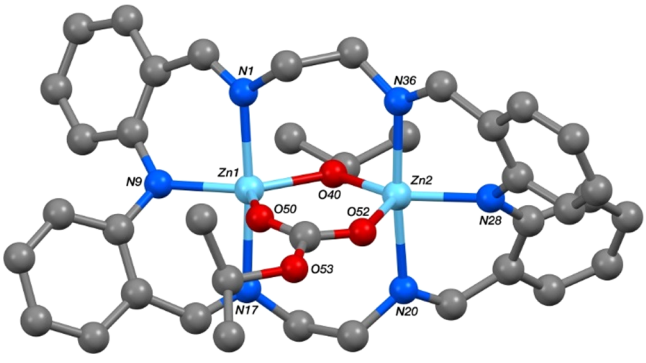

Figure 8. Structure of one (**3a-I**) of the two independent complexes present in the crystal of **3a**.

a CO_2-free atmosphere, by diffusion of hexane into a THF solution of the complex, under a N_2 atmosphere. It may be that, in the absence of a CO_2 atmosphere, there is a tendency for decarboxylation to form **3a**. In line with this proposal, degassing a solution containing **3b**, with subsequent removal of the volatile products, leads to formation of the bis(alkoxide) complex **2**, along with minor traces of decomposition products. These results suggest that there is an equilibrium between the alkoxide and carbonate species that can be perturbed by both temperature and CO_2. Indeed, related reversible CO_2 insertion was also observed by Coates and co-workers using zinc β-diiminate alkoxide complexes, although in that case, a higher pressure of CO_2 was required to access the carbonate.[28] Here, it is notable that the macrocycle complex is able to rapidly, and reversibly, insert CO_2 at 1 bar of pressure. In addition, the reaction of the zinc ethyl complex **1** with excess isopropyl alcohol (10 equiv) and 1 bar of CO_2 pressure leads to the same carbonate products as those obtained by reaction of the isolated alkoxide derivative **2** with CO_2. This suggests that formation of the carbonate species is likely to occur during the attempted catalysis using **1** and the failure to function as a catalyst relates to the reaction between the carbonate and epoxide rather than a failure to insert CO_2. Another interesting observation is the isolation of crystals of the zinc carbonate−alkoxide complex. In the previous study of CO_2 in a zinc alkoxide derivative, Coates and co-workers isolated a carbonate−alkoxide complex also [rather than the bis(carbonate) species].[28] They proposed that this species was a resting state in catalysis, and this was subsequently supported by a detailed theoretical study carried out by Rieger and co-workers, using the tethered β-diiminate complexes, which showed a high stability for such mixed carbonate−alkoxide intermediates.[41]

The structure of **3a** was found to contain two crystallographically independent complexes, **3a-I** and **3a-II**. While complex **3a-I** sits in a general position, complex **3a-II** is situated across a C_2 axis (which bisects the Zn3···Zn3A, N61···N61A, and N77···N77A vectors). Unfortunately, both the isopropoxide and carbonate bridging ligands are disordered about this axis, rendering the Zn−O bond lengths unreliable. Otherwise, all bonding and geometrical parameters for complexes **3a-I** and **3a-II** are as expected and are in line with the those of the structure of complex **2**, featuring a relatively planar central structure and twisted phenyl rings (57.52−64.62°).

Overall, the most obvious difference across all four complexes is a marked change in the conformation of the N_6 macrocycle on going from terminal coligands in **1** (Figure 2) to bridging coligands in **2** (Figure 6) and **3a-I**/**3a-II** (Figure 8). The length and width of the macrocycle as measured by the N9···N28, N1···N7, and N20···N36 separations are given in Table 1 and show how the introduction of bridging ligands shortens and widens the macrocycle in **2** and **3a-I**/**3a-II** compared to the conformation with terminal coligands seen in **1** [N9···N28 (head units) = 8.339(3) Å in **1** compared to 6.960(3)−7.330(5) Å in **2** and **3a-I**/**3a-II**; imines N1···N17 and N20···N36 = 3.386(2) and 3.352(2) Å in **1** compared to 4.319(4)−4.386(3) Å in **2** and **3a-I**/**3a-II**]. The acetate coligands in the previously reported $[L^{Et/Pr/Bu}Cu^{II}_2(OAc)_2]$ derivatives are terminal not bridging, so similar to complex **1**, the head unit N···N separations are long, ranging from 5.211 to 8.201 to 7.077 Å as the length of the linker is increased, and correspondingly the Cu···Cu separations range from 3.607 to 5.265 to 5.838 Å: the pairs of imine N···N separations for these three complexes fall in a tighter range, 3.810−3.827 Å.[50] Associated with the change from terminal to bridging coligands is a shortening of the Zn···Zn separation from 5.0270(4) Å in **1** to 2.9448(4) Å in **2**, 3.2062(5) Å in **3a-I**, and 3.3337(8) Å in **3a-II**. In each of **1**, **2**, and **3a-I**/**3a-II**, the Zn−N bonds to the amino nitrogen atoms N9 and N28 are shorter than those to the imino nitrogen atoms N1, N17, N20, and N36, as was seen in the previously reported $[L^{Et/Pr/Bu}Cu^{II}_2(OAc)_2]$ complexes,[50]

DOI: 10.1021/acs.inorgchem.5b02038
Inorg. Chem. 2015, 54, 11842−11851

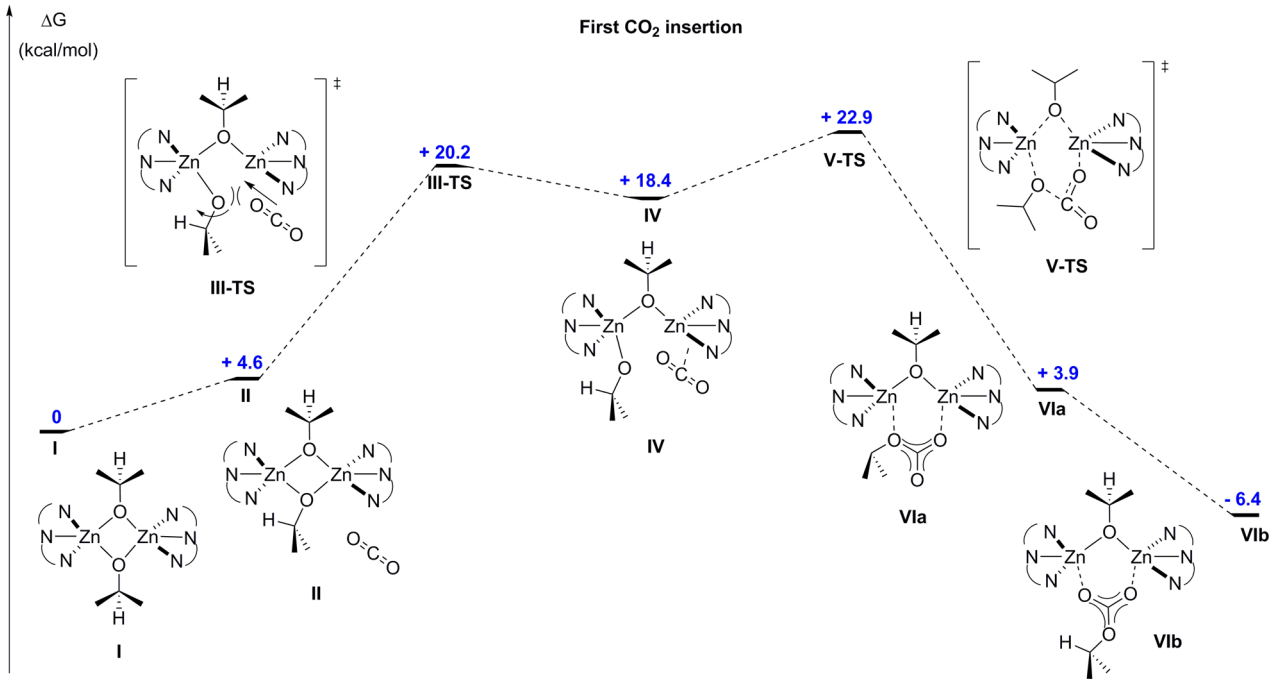

Figure 9. Potential energy surface for the first CO_2 insertion reaction between **2** (labeled **I** here) and one CO_2 molecule, forming **3a** (labeled **VIb** here). The ancillary ligand structure is omitted for clarity. DFT protocol: ωb97XD/6-31G(d)/scrf(cpcm = benzene); 298 K.

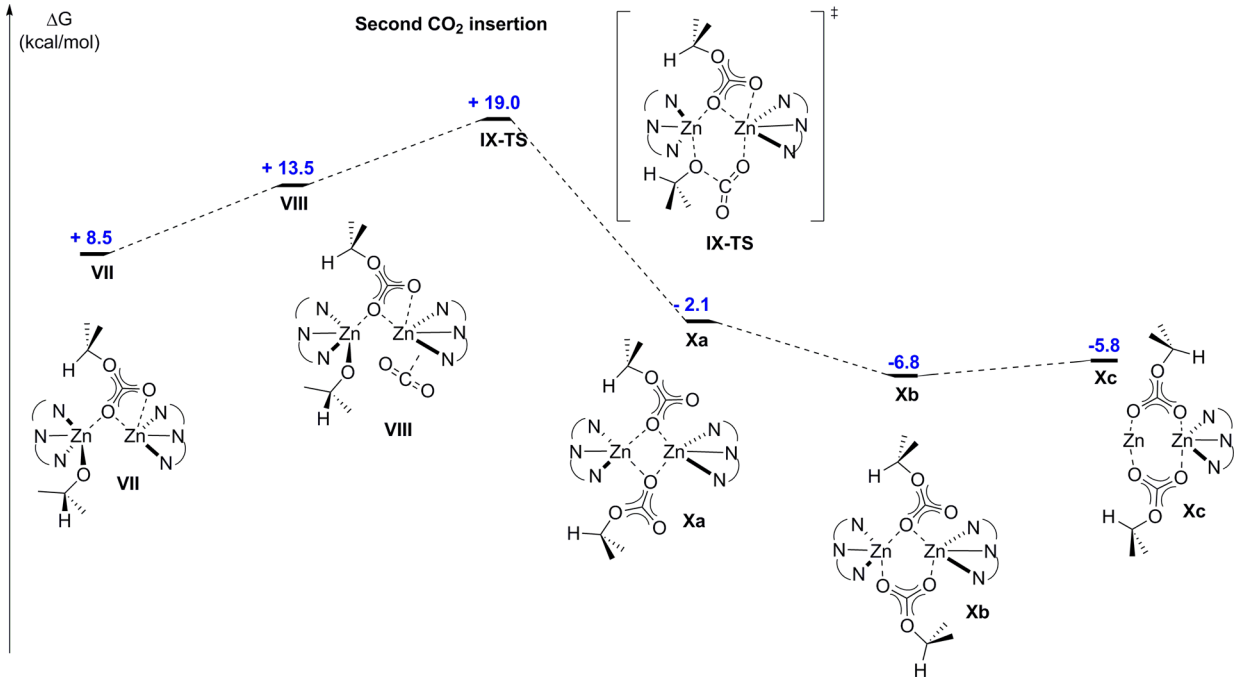

Figure 10. Potential energy surface for the second insertion reaction between **2** and one CO_2 molecule, i.e., insertion of one CO_2 into **3a** to form **3b** (labeled **Xc** here). The ancillary ligand structure is omitted for clarity. DFT protocol: ωb97xd/6-31G(d)/scrf(cpcm = benzene); 298 K.

and across **2** and **3a-I**, the Zn−O bonds to the alkoxide ligands are shorter than those to the carbonate ligand (with **3a-II** excluded because of the disorder discussed above).

In order to get a better understanding of the insertion of CO_2 into the zinc alkoxide bonds, a theoretical study using DFT calculations was carried out. The free energy profile, including the key transition states, was calculated for the reaction between **2** and 2 equiv of CO_2 (Figures 9 and 10). The calculations were carried out using the protocol ωb97XD/6-31G(d)/srcf(cpcm = benzene), which in previous related studies of dinuclear zinc complexes for similar reactions showed a good agreement with experiments.[34] The calculations reveal that the first CO_2 insertion into one of the zinc alkoxide bonds leads to compound **3a** (structure **VIb** in Figure 9). The second CO_2 insertion leads to formation of the bis(carbonate) complex **3b** (intermediates **Xa**−**c**; Figure 10).

The reference point for the calculations is complex **I** (compound **2**) with two molecules of CO_2, whose structure

DOI: 10.1021/acs.inorgchem.5b02038
Inorg. Chem. 2015, 54, 11842−11851

was calculated from the atomic coordinates available from the solid-state structure of **2**. The CO_2 approach to one of the faces of the complex concomitantly leads to decoordination of one of the bridging alkoxide groups to form intermediate **IV** via **III-TS** at $\Delta G = \pm 20.2$ kcal·mol^{-1} (see Figure S14). The calculations suggest that there are noncovalent interactions between CO_2 and the zinc imine moiety, which orients the CO_2 orthogonal to the alkoxide group (see Figure S15).[34]

It is notable that decoordination of the μ-alkoxide group to form **IV** is thermodynamically unfavorable, reenforcing the relative stability of **I** (compound **2**). However, the favorable orientation of CO_2 in intermediate **IV** facilitates access to the transition state **V-TS** ($\Delta\Delta G = +4.5$ kcal·mol^{-1}; overall barrier $\Delta G = +22.9$ kcal·mol^{-1}), where the alkoxide group attacks the carbon atom of CO_2. Concurrently, the CO_2 molecule rotates so as to allow carbonate coordination at the metal center, i.e., formation of the intermediate **VIa.** The formation of **VIa**, from **IV** via **V-TS**, has been confirmed by intrinsic reaction coordinate (IRC) calculations (Figure S16). Subsequent decoordination and reorientation of the carbonate group leads to various thermodynamically favored structures including structure **VIb** ($\Delta G = -6.4$ kcal·mol^{-1}), which has the same structure as the isolated crystals of complex **3a**.

The next step is to investigate the second CO_2 insertion, into the remaining alkoxide bond in **VIb**, the structure of which was calculated from the atomic coordinates of **3a** (determined by X-ray crystallography). Again the insertion of CO_2 occurs by decoordination of the μ-alkoxide group, accompanied by rotation of the carbonate group, leading to intermediate **VII** ($\Delta G = +8.5$ kcal·mol^{-1}), which has a coordinative vacancy at the zinc center. The next step involves the direct coordination of CO_2 to the zinc center, leading to intermediate **VIII**, where the CO_2 molecule is oriented orthogonal to the alkoxide group (Figure S18). The attack by the alkoxide group on the coordinated CO_2 leads to formation of the bis(carbonate) intermediate, **Xa**, via a relatively low-energy transition state ($\Delta G^{TS} = 19.0$ kcal·mol^{-1} and $\Delta\Delta G = 25.4$ kcal·mol^{-1} from **VIb**). The formation of **Xa**, from **VIII** via **IX-TS**, was confirmed by IRC calculations (Figure S17). Subsequent decoordination and rotation of the carbonate groups lead to various isomers, including structure **VIIIb** ($\Delta G = -6.8$ kcal·mol^{-1}), featuring one bridging κ^2-carbonate group and one μ-carbonate group.

In both steps, the relatively low-energy barriers for CO_2 insertions (<25 kcal·mol^{-1}) are in accordance with the experimental results, where insertion of CO_2 occurs at room temperature and 1 bar of pressure. It is proposed that the dinuclearity of the complex is important in stabilizing CO_2 insertion by allowing its favorable orientation relative to the alkoxide group and, at the same time, by stabilizing the carbonate species formed by enabling it to bridge between the two metal centers. It is also notable that various zinc carbonate isomers (**VIa,b** and **Xa−c**) are observed by DFT, each featuring different coordination modes of the carbonate groups and all with somewhat similar relative energies, which may go some way to explaining the mixture of carbonate species observed by ^{1}H NMR spectroscopy.

CONCLUSIONS

In conclusion, the high yielding synthesis and reactivity of the dizinc(II) bis(alkyl) complex **1**, coordinated by a Schiff base macrocyclic ancillary ligand, are reported. The dizinc bis(alkyl) complex reacts with isopropyl alcohol, at slightly elevated temperatures, to form the dizinc bis(isopropoxide) complex **2**, which has been fully characterized, including by X-ray crystallography. The alkoxide derivative (**2**) is a good model for the propagating species during lactide ROP, and indeed, the alkyl complex, in the presence of isopropyl alcohol, is a moderately efficient and well-controlled catalyst for *rac*-LA polymerization. The same catalytic system, however, is not able to copolymerize cyclohexene oxide/CO_2, despite showing rapid and reversible insertion of CO_2 into the zinc alkoxide moieties. The stoichiometric reaction between the dizinc bis(alkoxide) derivative and 1 bar of CO_2 leads to the evolution of dizinc carbonate moieties (**3a** and **3b**) as established by NMR spectroscopy and a carbonate alkoxide derivative characterized by X-ray crystallography. The insertion of CO_2 into the dizinc bis(alkoxide) species is also studied using DFT, which reveals that there are low barriers to insertion and that the reaction could proceed in a stepwise manner, forming a relatively stable dizinc carbonate−alkoxide intermediate.

Overall, this study confirms that using this new type of dinucleating macrocycle may indeed be a useful strategy to prepare zinc alkoxide derivatives that are suitable as lactone ROP catalysts and that undergo rapid insertion of CO_2 at 1 bar of pressure. Further work is necessary to optimize the coordination environment so as to enable efficient CO_2/epoxide copolymerization, and this will be the focus of future activities.

EXPERIMENTAL SECTION

Materials and Methods. All reactions were conducted under an atmosphere of dry N_2, using standard Schlenk-line techniques, and in a nitrogen-filled glovebox. Solvents and reagents were obtained from commercial sources (Sigma-Aldrich). The metal-free Schiff base macrocycle H_2L was prepared as described previously.[50] Tetrahydrofuran (THF), toluene, and hexane were distilled from sodium/benzophenone, under dry N_2. Cyclohexane oxide was dried over 3 Å molecular sieves. *rac*-lactide (*rac*-LA) was crystallized from anhydrous toluene and sublimed under vacuum two times prior to use.

NMR spectra were recorded on a Bruker AV400 instrument. The residual proteo solvent peaks were used as internal references in the ^{1}H and ^{13}C NMR spectra (ppm). Homonuclear-decoupled ^{1}H{^{1}H} NMR spectra were performed on a Bruker Av500 spectrometer, equipped with a z-gradient bbo/5 mm tunable probe and a BSMS GAB 10 A gradient amplifier providing a maximum gradient output of 5.35 G·cmA^{-1}. ^{1}H NMR spectra for all lactide polymerizations were performed on a Bruker Av400 or Av500 instrument. PLA number-averaged MW, M_n, and dispersities (M_w/M_n; $Đ$) were determined using size-exclusion chromatography. Two mixed-bed PSS−SDV linear S columns were used in series, with THF as the eluent, at a flow rate of 1 mL·min^{-1}, on a Shimadzu LC-20AD instrument operating at 40 °C. The instrument was calibrated using narrow MW polystyrene standards, and a correction factor of 0.58 was applied to the raw MW data, as reported by Penczek and co-workers.[68,69] MALDI-ToF spectrometry measurements were performed on Waters/Micromass MALDI micro MX spectrometer, using positive ionization in reflectron mode. The samples were prepared by dissolving the polymers, the dithranol matrix, and potassium trifluoroacetate, as the cationizing agent, in a 1:1:1 ratio, in THF (all solutions being at 10 mg·mL^{-1}).

Computational Details. All calculations were performed using the *Gaussian09* suite of codes (revision C.01). Calculations were carried out at the DFT level of theory, using hybrid functional ωB97XD. All atoms, including zinc, have been described with a 6-31G(d) basis set. Geometry optimizations were carried out without any symmetry restrictions. Conductor-like polarizable continuum model (CPCM) was used with benzene as the solvent to model solvation. The nature of the *extrema* was verified with analytical frequency calculations: the stationary points (*minima*) do not feature imaginary modes, and all transition states reveal precisely one imaginary mode corresponding to

DOI: 10.1021/acs.inorgchem.5b02038
Inorg. Chem. 2015, 54, 11842−11851

the intended reaction. For **III-TS** and **VII-TS**, IRC calculations were performed, which also confirmed the identity of the transition state.

Complex Syntheses. *LZn_2Et_2 (1).* A $ZnEt_2$ (99.1 mg, 0.80 mmol) solution, in THF (4 mL, −40 °C), was added to a precooled suspension of H_2L (200 mg, 0.40 mmol), in THF (5 mL, −40 °C). The mixture slowly turned red and became homogeneous after 30 min. The solution was allowed to react at 25 °C for 10 h. Then, the volatile components were evaporated, the residue was washed (pentane), and compound **1** was isolated as a red solid (241 mg, 87%). Suitable crystals of **1**·C_6H_6 for X-ray analysis were obtained by hexane diffusion into a benzene solution of **1**. Elem anal. Calcd: C, 63.03; H, 5.59; N, 12.26. Found: C, 63.09; H, 5.60; N, 12.23. ^{1}H NMR (400 MHz, C_6D_6): δ 7.36 (s, 4 H, N=C*H*), 7.26 (d, ^3J = 8 Hz, 4 H, aryl-*H*), 6.96 (ddd, ^3J = 8 Hz, ^3J = 8 Hz, ^5J = 2 Hz, 4 H, aryl-*H*), 6.71 (d, ^3J = 8 Hz, 4 H, aryl-*H*), 6.50 (dd, ^3J = 8 Hz, ^3J = 8 Hz, 4 H, aryl-*H*), 3.86 (dd, ^2J = 12 Hz, ^3J = 6 Hz, 4 H, C$H_aH_{a'}$), 2.74 (dd, ^2J = 12 Hz, ^3J = 6 Hz, 4 H, C$H_aH_{a'}$), 1.38 (t, ^3J = 8 Hz, 6 H, $ZnCH_2CH_3$), 0.34 (q, ^3J = 8 Hz, 4 H, $ZnCH_2CH_3$). ^{13}C{^{1}H} NMR (100 MHz, C_6D_6): δ 168.5 (CH, N=*C*H), 154.2 (C_{quat}, aryl), 136.4 (CH, aryl), 132.7 (CH, aryl), 122.9 (br C_{quat}, aryl), 120.0 (br CH, aryl), 117.4 (br CH, aryl), 61.9 (CH_2, NCH_2), 14.1 (CH_3, Zn*Et*), −2.8 (CH_2, Zn*Et*).

$L^{Et}Zn_2(O^iPr)_2$ (2). In situ method (reaction monitoring): In a J. Young NMR tube, a slight excess of isopropyl alcohol (2.5 μL, 0.032 mmol.) was added to a THF solution (0.6 mL) of **1** (10 mg, 0.014 mmol.). The reaction was monitored at 25 °C for 20 h and then heated at 60 °C for 16 h, which leads to the formation of **2**. Suitable crystals for X-ray analysis were obtained by hexane diffusion into a THF solution of **2**. ^{1}H NMR (400 MHz, THF-d_8): δ 8.32 (s, 4 H, N=C*H*), 7.22 (dd, ^3J = 8 Hz, ^4J = 1.2 Hz, 4H, aryl-*H*), 6.93 (ddd, ^3J = 8 Hz, ^3J = 8 Hz, ^4J = 1.2 Hz, 4 H, aryl-*H*), 6.90 (d, ^3J = 8 Hz, 4 H, aryl-*H*), 6.58 (dd, ^3J = 8 Hz, ^3J = 8 Hz, 4 H, aryl-*H*), 4.13 (m, 4 H, CH_2), 3.85−3.78 (m, 6 H, CH_2 + O^{i}Pr), 0.61 (d, ^3J = 5.5 Hz, 6 H, O^{i}Pr), 0.60 (d, ^3J = 5.5 Hz, 6 H, O^{i}Pr). ^{13}C{^{1}H} NMR (100 MHz, THF-d_8): δ 167.7 (CH, N=*C*H), 157.6 (C_{quat}, aryl), 134.5 (CH, aryl), 131.1 (CH, aryl), 124.3 (br CH, aryl), 123.9 (C_{quat}, aryl), 116.9 (br CH, aryl), 65.0 (CH_2, NCH_2), 63.4 (CH, O^{i}Pr), 28.1 (CH_3, O^{i}Pr).

Isolated Sample. In a sealed vial, isopropyl alcohol (167 μL, 2.18 mmol) was added to a THF solution (10 mL) of **1** (150 mg, 0.22 mmol). The mixture was stirred at 25 °C for 1 h, before being heated at 60 °C for 16 h. The solution was concentrated, and then hexane (15 mL) was added, which led to the formation of a yellow precipitate, which was filtered, washed (hexane), and dried to yield **2** as a yellow powder (45 mg, 27%). Elem anal. Calcd: C, 61.22; H, 5.68; N, 11.27. Found: C, 60.96; H, 5.78; N, 11.16. ^{1}H NMR (400 MHz, C_6D_6): δ 7.90 (s, 4 H, N=C*H*), 7.27 (d, ^3J = 8.6 Hz, 4 H, aryl-*H*), 7.13 (dd, ^3J = 7.7 Hz, ^4J = 1.2 Hz, 4 H, aryl-*H*), 6.95 (ddd, ^3J = 8.6 Hz, ^3J = 6.8 Hz, ^4J = 1.8 Hz, 4 H, aryl-*H*), 6.66 (ddd, ^3J = 7.7 Hz, ^3J = 6.6 Hz, ^4J = 1.0 Hz, 4 H, aryl-*H*), 4.00−3.92 (m, 4H, CH_2), 3.89 (sept, ^3J = 6.0 Hz, 2 H, O^{i}Pr), 3.22−3.10 (m, 4 H, CH_2), 0.87 (d, ^3J = 6.0 Hz, 6 H, O^{i}Pr). ^{13}C{^{1}H} NMR (100 MHz, C_6D_6): δ 166.9 (CH, N=CH), 157.5 (C_{quat}, aryl), 134.3 (CH, aryl), 131.5 (CH, aryl), 124.4 (br CH, aryl), 123.4 (C_{quat}, aryl), 117.0 (br CH, aryl), 65.2 (CH, O^{i}Pr), 64.5 (CH_2, NCH_2), 28.2 (CH_3, O^{i}Pr), 28.1 (CH_3, O^{i}Pr).

$L^{Et}Zn_2(OCOO^iPr)_2$ (3b). From Compound 2. In a J. Young NMR tube, **2** (10 mg, 0.013 mmol) was dissolved in C_6D_6 (0.6 mL). The solution was frozen and subjected to a vacuum, and then CO_2 was added at 1 bar of pressure. The solution was allowed to react at 25 °C, for 10 min, and then the NMR spectra were recorded, which showed the formation of a product having carbonate signals. ^{1}H NMR (400 MHz, C_6D_6): δ 7.72 (s, 4 H, N=C*H*), 7.50 (d, ^3J = 8 Hz, 4 H, aryl-*H*), 7.00 (dd, ^3J = 8 Hz, ^4J = 1.6 Hz, 4 H, aryl-*H*), 6.95 (ddd, ^3J = 8 Hz, ^3J = 8 Hz, ^4J = 1.6 Hz, 4 H, aryl-*H*), 6.62 (dd, ^3J = 8 Hz, ^3J = 8 Hz, 4 H, aryl-*H*), 4.47 (hept, ^3J = 6.2 Hz, 2 H, O^{i}Pr), 3.74−3.64 (m, 8H, CH_2), 0.72 (d, ^3J = 6.2 Hz, 12 H, O^{i}Pr). ^{13}C{^{1}H}NMR (100 MHz, C_6D_6): δ 168.7 (CH, N=*C*H), 157.8 (C_{quat}, carbonate OCOO^{i}PR), 156.6 (C_{quat}, aryl), 135.5 (CH, aryl), 131.9 (CH, aryl), 123.3 (CH, aryl), 122.7 (C_{quat}, aryl), 117.1 (CH, aryl), 69.4 (CH, O^{i}Pr), 63.9 (CH_2, NCH_2), 25.5 (CH3, O^{i}Pr).

From Compound 1. In a J. Young NMR tube, **1** (10 mg, 0.015 mmol) was dissolved in C_6D_6 (0.6 mL), and an excess of isopropyl alcohol was added (11.1 μL, 0.15 mmol). The solution was frozen and subjected to a vacuum, and then CO_2 was added at 1 bar of pressure. The solution was allowed to react at 60 °C for 2 h, and then the NMR spectra were recorded, which showed the formation of **3b**, as previously observed. Suitable crystals for X-ray analysis were obtained by hexane diffusion into the C_6D_6 solution in the glovebox, under a N_2 atmosphere. The crystals were found to be **3a**.

■ ASSOCIATED CONTENT

Ⓢ Supporting Information

The Supporting Information is available free of charge on the ACS Publications website at DOI: 10.1021/acs.inorgchem.5b02038.

NMR spectra, XYZ files for structure I−X, web-enhanced features, and complete computational, experimental, and X-ray crystallographic details (PDF)
X-ray crystallographic data in CIF format (CIF)
Sequential CO2 insertion (HTML)

■ AUTHOR INFORMATION

Corresponding Authors

*E-mail: c.k.williams@imperial.ac.uk.
*E-mail: sbrooker@chemistry.otago.ac.nz.

Notes

The authors declare no competing financial interest.

■ ACKNOWLEDGMENTS

The University of Otago, the MacDiarmid Institute for Advanced Materials and Nanotechnology, and the EPSRC (Grants EP/EP/L017393/1, EP/K035274, EP/K014070/1) are acknowledged for research funding. We thank Imperial College London HPC for computing resources.

■ REFERENCES

(1) Matsunaga, S.; Shibasaki, M. *Chem. Commun.* **2014**, *50*, 1044.
(2) Pérez-Temprano, M. H.; Casares, J. A.; Espinet, P. *Chem. - Eur. J.* **2012**, *18*, 1864.
(3) Anbu, S.; Kamalraj, S.; Varghese, B.; Muthumary, J.; Kandaswamy, M. *Inorg. Chem.* **2012**, *51*, 5580.
(4) Jarenmark, M.; Kappen, S.; Haukka, M.; Nordlander, E. *Dalton Trans.* **2008**, 993.
(5) Kaminskaia, N. V.; He, C.; Lippard, S. J. *Inorg. Chem.* **2000**, *39*, 3365.
(6) Leeland, J. W.; Finn, C.; Escuyer, B.; Kawaguchi, H.; Nichol, G. S.; Slawin, A. M. Z.; Love, J. B. *Dalton Trans.* **2012**, *41*, 13815.
(7) Pankhurst, J. R.; Cadenbach, T.; Betz, D.; Finn, C.; Love, J. B. *Dalton Trans.* **2015**, *44*, 2066.
(8) Kember, M. R.; Buchard, A.; Williams, C. K. *Chem. Commun.* **2011**, *47*, 141.
(9) Romain, C.; Thevenon, A.; Saini, P. K.; Williams, C. K. In *Topics in Organometallic Chemistry: Carbon Dioxide and Organometallics*; Lu, X. B., Ed.; Springer: Berlin, 2015.
(10) Paul, S.; Zhu, Y. Q.; Romain, C.; Saini, P. K.; Brooks, R.; Williams, C. K. *Chem. Commun.* **2015**, *51*, 6459.
(11) Ajellal, N.; Carpentier, J. F.; Guillaume, C.; Guillaume, S. M.; Helou, M.; Poirier, V.; Sarazin, Y.; Trifonov, A. *Dalton Trans.* **2010**, *39*, 8363.
(12) Buffet, J.-C.; Okuda, J. *Polym. Chem.* **2011**, *2*, 2758.
(13) Dijkstra, P. J.; Du, H. Z.; Feijen, J. *Polym. Chem.* **2011**, *2*, 520.
(14) Tschan, M. J. L.; Brule, E.; Haquette, P.; Thomas, C. M. *Polym. Chem.* **2012**, *3*, 836.
(15) Williams, C. K.; Hillmyer, M. A. *Polym. Rev.* **2008**, *48*, 1.
(16) Darensbourg, D. J.; Yeung, A. D. *Polym. Chem.* **2014**, *5*, 3949.
(17) Childers, M. I.; Longo, J. M.; Van Zee, N. J.; LaPointe, A. M.; Coates, G. W. *Chem. Rev.* **2014**, *114*, 8129.

DOI: 10.1021/acs.inorgchem.5b02038
Inorg. Chem. 2015, 54, 11842−11851

(18) Wu, G. P.; Darensbourg, D. J.; Lu, X. B. *J. Am. Chem. Soc.* **2012**, *134*, 17739.
(19) Inkinen, S.; Hakkarainen, M.; Albertsson, A. C.; Sodergard, A. *Biomacromolecules* **2011**, *12*, 523.
(20) Guillaume, S. M.; Kirillov, E.; Sarazin, Y.; Carpentier, J.-F. *Chem. - Eur. J.* **2015**, *21*, 7988.
(21) von der Assen, N.; Bardow, A. *Green Chem.* **2014**, *16*, 3272.
(22) Chapman, A. C.; Keyworth, C.; Kember, M. R.; Lennox, A. J. J.; Williams, C. K. *ACS Catal.* **2015**, *5*, 1581.
(23) Inoue, S. *J. Polym. Sci., Part A: Polym. Chem.* **2000**, *38*, 2861.
(24) Inoue, S.; Koinuma, H.; Tsuruta, T. *J. Polym. Sci., Part B: Polym. Lett.* **1969**, *7*, 287.
(25) Darensbourg, D. J.; Mackiewicz, R. M.; Rodgers, J. L.; Fang, C. C.; Billodeaux, D. R.; Reibenspies, J. H. *Inorg. Chem.* **2004**, *43*, 6024.
(26) Darensbourg, D. J.; Wildeson, J. R.; Yarbrough, J. C.; Reibenspies, J. H. *J. Am. Chem. Soc.* **2000**, *122*, 12487.
(27) Darensbourg, D. J.; Holtcamp, M. W. *Macromolecules* **1995**, *28*, 7577.
(28) Moore, D. R.; Cheng, M.; Lobkovsky, E. B.; Coates, G. W. *J. Am. Chem. Soc.* **2003**, *125*, 11911.
(29) Bok, T.; Yun, H.; Lee, B. Y. *Inorg. Chem.* **2006**, *45*, 4228.
(30) Lee, B. Y.; Kwon, H. Y.; Lee, S. Y.; Na, S. J.; Han, S. I.; Yun, H. S.; Lee, H.; Park, Y. W. *J. Am. Chem. Soc.* **2005**, *127*, 3031.
(31) Saini, P. K.; Romain, C.; Zhu, Y.; Williams, C. K. *Polym. Chem.* **2014**, *5*, 6068.
(32) Kember, M. R.; Williams, C. K. *J. Am. Chem. Soc.* **2012**, *134*, 15676.
(33) Kember, M. R.; Jutz, F.; Buchard, A.; White, A. J. P.; Williams, C. K. *Chem. Sci.* **2012**, *3*, 1245.
(34) Buchard, A.; Jutz, F.; Kember, M. R.; White, A. J. P.; Rzepa, H. S.; Williams, C. K. *Macromolecules* **2012**, *45*, 6781.
(35) Jutz, F.; Buchard, A.; Kember, M. R.; Fredriksen, S. B.; Williams, C. K. *J. Am. Chem. Soc.* **2011**, *133*, 17395.
(36) Buchard, A.; Kember, M. R.; Sandeman, K. G.; Williams, C. K. *Chem. Commun.* **2011**, *47*, 212.
(37) Kember, M. R.; White, A. J. P.; Williams, C. K. *Macromolecules* **2010**, *43*, 2291.
(38) Kember, M. R.; Knight, P. D.; Reung, P. T. R.; Williams, C. K. *Angew. Chem., Int. Ed.* **2009**, *48*, 931.
(39) Kissling, S.; Lehenmeier, M. W.; Altenbuchner, P. T.; Kronast, A.; Reiter, M.; Deglmann, P.; Seemann, U. B.; Rieger, B. *Chem. Commun.* **2015**, *51*, 4579.
(40) Piesik, D. F. J.; Range, S.; Harder, S. *Organometallics* **2008**, *27*, 6178.
(41) Kissling, S.; Altenbuchner, P. T.; Lehenmeier, M. W.; Herdtweck, E.; Deglmann, P.; Seemann, U. B.; Rieger, B. *Chem. - Eur. J.* **2015**, *21*, 8148.
(42) Lehenmeier, M. W.; Kissling, S.; Altenbuchner, P. T.; Bruckmeier, C.; Deglmann, P.; Brym, A.-K.; Rieger, B. *Angew. Chem., Int. Ed.* **2013**, *52*, 9821.
(43) Piesik, D. F. J.; Haack, P.; Harder, S.; Limberg, C. *Inorg. Chem.* **2009**, *48*, 11259.
(44) Piesik, D. F. J.; Stadler, R.; Range, S.; Harder, S. *Eur. J. Inorg. Chem.* **2009**, *2009*, 3569.
(45) Platel, R. H.; Hodgson, L. M.; Williams, C. K. *Polym. Rev.* **2008**, *48*, 11.
(46) Williams, C. K.; Brooks, N. R.; Hillmyer, M. A.; Tolman, W. B. *Chem. Commun.* **2002**, 2132.
(47) Yao, W.; Mu, Y.; Gao, A.; Gao, W.; Ye, L. *Dalton Trans.* **2008**, 3199.
(48) Chen, C.-T.; Chan, C.-Y.; Huang, C.-A.; Chen, M.-T.; Peng, K.-F. *Dalton Trans.* **2007**, 4073.
(49) Otero, A.; Fernández-Baeza, J.; Sánchez-Barba, L. F.; Tejeda, J.; Honrado, M.; Garcés, A.; Lara-Sánchez, A.; Rodríguez, A. M. *Organometallics* **2012**, *31*, 4191.
(50) Cameron, S. A.; Brooker, S. *Inorg. Chem.* **2011**, *50*, 3697.
(51) Black, D.; Rothnie, N. *Aust. J. Chem.* **1983**, *36*, 2395.
(52) Black, D. S. C.; Rothnie, N. E. *Tetrahedron Lett.* **1978**, *19*, 2835.
(53) Sanyal, R.; Cameron, S. A.; Brooker, S. *Dalton Trans.* **2011**, *40*, 12277.
(54) Ansell, C. W. G.; Lewis, J.; Raithby, P. R. *J. Chem. Soc., Dalton Trans.* **1982**, 2557.
(55) Wilson, R. K.; Brooker, S. *Dalton Trans.* **2013**, *42*, 7913.
(56) Wilson, R. K.; Brooker, S. *Dalton Trans.* **2013**, *42*, 12075.
(57) Romain, C.; Rosa, V.; Fliedel, C.; Bier, F.; Hild, F.; Welter, R.; Dagorne, S.; Aviles, T. *Dalton Trans.* **2012**, *41*, 3377.
(58) Yang, L.; Powell, D. R.; Houser, R. P. *Dalton Trans.* **2007**, 955.
(59) Brooker, S. *Coord. Chem. Rev.* **2001**, *222*, 33.
(60) Brooker, S.; Croucher, P. D.; Roxburgh, F. M. *J. Chem. Soc., Dalton Trans.* **1996**, 3031.
(61) Arbaoui, A.; Redshaw, C. *Polym. Chem.* **2010**, *1*, 801.
(62) Wang, L.; Poirier, V.; Ghiotto, F.; Bochmann, M.; Cannon, R. D.; Carpentier, J.-F.; Sarazin, Y. *Macromolecules* **2014**, *47*, 2574.
(63) Wang, L.; Bochmann, M.; Cannon, R. D.; Carpentier, J.-F.; Roisnel, T.; Sarazin, Y. *Eur. J. Inorg. Chem.* **2013**, *2013*, 5896.
(64) Addison, A. W.; Rao, T. N.; Reedijk, J.; van Rijn, J.; Verschoor, G. C. *J. Chem. Soc., Dalton Trans.* **1984**, 1349.
(65) Brombacher, H.; Vahrenkamp, H. *Inorg. Chem.* **2004**, *43*, 6042.
(66) Kato, M.; Ito, T. *Inorg. Chem.* **1985**, *24*, 509.
(67) Ruf, M.; Vahrenkamp, H. *Inorg. Chem.* **1996**, *35*, 6571.
(68) Kowalski, A.; Duda, A.; Penczek, S. *Macromolecules* **1998**, *31*, 2114.
(69) Save, M.; Schappacher, M.; Soum, A. *Macromol. Chem. Phys.* **2002**, *203*, 889.

DOI: 10.1021/acs.inorgchem.5b02038
Inorg. Chem. 2015, 54, 11842−11851